



E2F1 Mediates the Retinoic Acid-Induced Transcription of *Tshz1* during Neuronal Differentiation in a Cell Division-Dependent Manner

Jo Hae Park,^a Kunsoo Rhee^a

^aDepartment of Biological Sciences, Seoul National University, Seoul, South Korea

ABSTRACT The involvement of cell division in cellular differentiation has long been accepted. Cell division may be required not only for the expansion of a differentiated cell population but also for the execution of differentiation processes. Nonetheless, knowledge regarding how specific differentiation processes are controlled in a cell division-dependent manner is far from complete. Here, we determined the involvement of cell division in neuronal differentiation. We initially confirmed that cell division is an essential event for the neuronal differentiation of P19 embryonic carcinoma cells. We investigated the induction mechanisms of *Tshz1*, whose expression is induced by retinoic acid (RA) in a cell division-dependent manner. Promoter analysis of *Tshz1* revealed a specific region required for RA-dependent transcription. A series of experiments was used to identify E2F1 as the induction factor for the RA-dependent transcription of *Tshz1*. We propose that E2F1 mediates neuronal differentiation in a cell division-dependent manner.

KEYWORDS cell division, neuronal differentiation, embryonic carcinoma cell, E2F, *Tshz1*

Cell division is tightly controlled during differentiation processes. In most cases, cell division is delayed and eventually ceases when cells undergo terminal differentiation. Additionally, cells have to divide for successful differentiation processes. Such cell division may be important not only for the expansion of a differentiated cell population but also for the execution of differentiation processes. In fact, cell division is essential for cell fate switches in pluripotent stem cells and for specific differentiation processes. One of the best examples may be the mitotic clonal expansion (MCE) event for adipocyte differentiation (1). MCE is two to three rounds of synchronous cell division that sequentially occur after the induction of signals for the onset of adipogenesis. MCE is required for the activation of *C/EBPβ* and the transcription of *C/EBPα* and peroxisome proliferator-activated receptor γ 2 (*PPARγ*), both of which are essential for ensuring adipocyte differentiation (2, 3). As expected, treatment with cell cycle blockers suppresses adipogenesis and MCE (4).

Several mechanisms have been suggested to explain how differentiation processes are controlled by cell division. First, a global restructuring of chromatin may be facilitated when cells go through the S phase and mitosis (5). During the S phase, reestablishing the chromatin state on newly synthesized DNA is potentially important for maintaining or switching cell identity. During the M phase, most transcription-associated factors dissociate from chromatin, and the cell-type-specific transcription programs temporarily halt. These changes could be critical for switching gene expression patterns favorable to differentiation. Second, cell fate decisions are frequently made during specific stages of the cell cycle. For example, human embryonic stem cells are determined to become endoderm in their early G₁ phase and to become neuroectoderm in their late G₁ phase (6). Third, cell cycle components directly control the expression of specific genes for differentiation (7). For example, cyclin D recruits

Received 3 May 2018 Returned for
modification 5 June 2018 Accepted 9
August 2018

Accepted manuscript posted online 13
August 2018

Citation Park JH, Rhee K. 2018. E2F1 mediates the retinoic acid-induced transcription of *Tshz1* during neuronal differentiation in a cell division-dependent manner. *Mol Cell Biol* 38:e00217-18. <https://doi.org/10.1128/MCB.00217-18>.

Copyright © 2018 American Society for Microbiology. All Rights Reserved.
Address correspondence to Kunsoo Rhee, rheek@snu.ac.kr.

transcriptional corepressors to endoderm genes and coactivators to neuroectoderm genes during the differentiation of human embryonic stem cells (8). It is likely that future research will reveal additional regulatory mechanisms for the cell division control of developmental processes.

In this study, we investigated the importance of cell division in neuronal differentiation. We used P19 cells, murine embryonic carcinoma cells that can efficiently differentiate into neurons in the presence of retinoic acid (RA) (9). We initiated the study by examining the differentiation efficiency of P19 cells upon blockage of cell cycle progression. Furthermore, we identified a factor whose activity is regulated in a cell division-dependent manner. Our results showed that the transcription of *Tshz1*, an upstream regulator of neuronal differentiation, is induced by E2F1, whose activity partially depends on cell division.

RESULTS

Effects of cell division blockers on the neuronal differentiation of P19 cells. P19 embryonic carcinoma cells have the potential to differentiate into diverse cell types, including neurons (9). RA allows P19 cells to form embryoid bodies (EBs) in a bacterial plate and then to differentiate into neuronal cells in a culture dish (Fig. 1A). To examine the importance of the early events that occur after RA treatment, we reduced the EB formation period and determined the number of cells that differentiated into neurons. The results showed that only 10% of P19 cells differentiated to form neurites when the EB formation period was shortened to 1 day (Fig. 1B and C). A period of at least 2 days of EB formation was required for efficient differentiation into neurons (Fig. 1B and C). To determine the importance of cell division in the early differentiation period of P19 cells, we treated the P19 cells with thymidine, an S phase blocker. The number of cells with neurites was significantly reduced after thymidine treatment (Fig. 1D and E). We also observed a similar result with RO3306, a G₂ phase blocker (data not shown). These results suggest that cell division at an early phase is an essential event for the efficient neuronal differentiation of P19 cells.

RA-induced expression of *Tshz1* during neuronal differentiation. RA is known to induce the expression of a group of genes required for the neuronal differentiation of P19 cells. The transcription of selected early genes are directly induced by retinoic acid-responsive elements (RAREs) within the promoters (10). The expression of secondary response genes follows, probably via actions of the mediating transcription factors (10). To test the hypothesis that cell division is required for neuronal differentiation, we decided to select a gene whose expression is induced by RA in a cell division-dependent manner. A list of candidate genes was obtained from previous proteomic analyses (11–13). From the gene pools, we identified 11 candidate genes whose expression levels were suppressed by thymidine treatment (data not shown). *Tshz1* was one of the RA-induced genes whose expression was significantly suppressed by cell cycle inhibitors. *Tshz1* is a zinc finger-type transcription factor that is involved in trunk patterning in *Drosophila* (14). *Tshz1* knockout mice display diverse defects in the nervous system, including malformation of the olfactory bulb (15). To determine the involvement of *Tshz1* in neuronal differentiation, we depleted *Tshz1* in P19 cells (Fig. 2A). The number of cells with neurites was significantly reduced in the *Tshz1*-depleted P19 cells (Fig. 2B and C). Therefore, we investigated how *Tshz1* expression is regulated during the neuronal differentiation of P19 cells.

Reverse transcription (RT)-PCR analysis revealed that *Tshz1* expression was induced by RA (Fig. 2D). *Tshz1* expression was not immediately induced by RA. Rather, *Tshz1* transcript levels gradually increased up to 24 h (Fig. 2E). The RA induction rate was suppressed after thymidine treatment (Fig. 2D and E). RO3306, another cell cycle blocker, also suppressed RA-induced *Tshz1* expression (Fig. 2F). These results suggest that RA-induced *Tshz1* expression partially depends on cell division.

RA-dependent activation of *Tshz1* transcription partially depends on cell division. We performed reporter gene assays to identify the essential region for the transcriptional activation of *Tshz1* in P19 cells. RA treatment induced luciferase activity

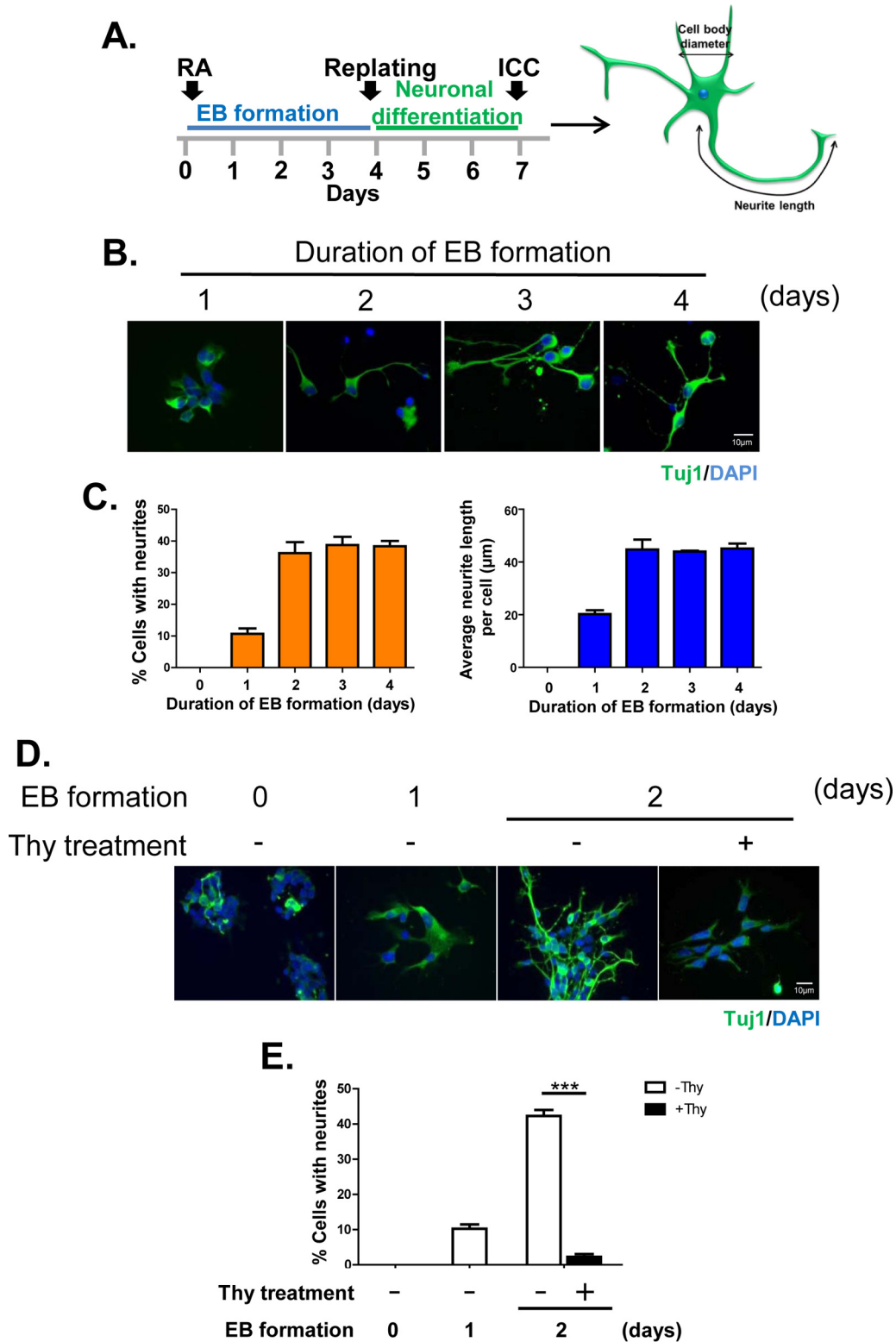


FIG 1 Effects of a cell division blocker on the neuronal differentiation of P19 cells. (A) P19 cells were treated with RA and cultured in a bacterial plate to induce EB formation. The cells were then replated in a tissue culture dish, cultured for 4 days, and immunostained with the Tuj1 antibody to determine neuronal differentiation. (B) The RA-treated P19 cells were cultured in bacterial plates for the indicated time periods and then transferred to culture dishes to induce neuronal differentiation. Three days later, the cells were immunostained with the Tuj1 antibody (green). DNA was stained with DAPI (blue). Bar, 10 μm . (C) The number of cells with neurites and the average neurite length per cell were analyzed. More than 100 cells were quantified. Data are shown as the means and SD ($n = 3$). (D) The RA-treated P19 cells were treated with thymidine and cultured for 2 days in a bacterial plate. The cells were then replated, cultured for 3 days, and immunostained

(Continued on next page)

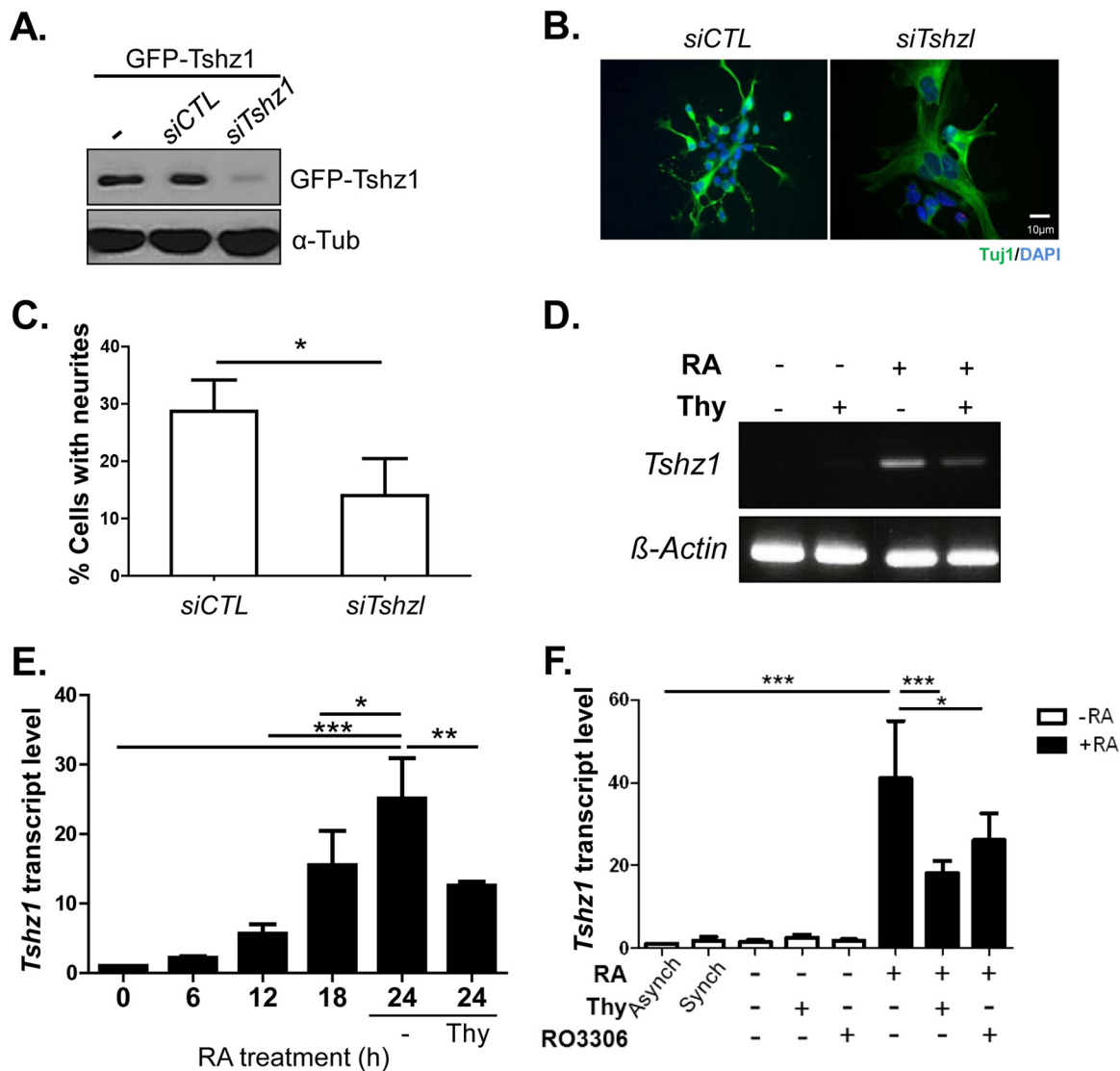


FIG 2 RA induction of *Tshz1* expression. (A) GFP-Tshz1-overexpressing P19 cells were transfected with siTshz1 and cultured for 48 h. Immunoblot analysis was performed with antibodies specific to GFP and α -tubulin. (B) Neuronal differentiation was induced in Tshz1-depleted P19 cells. The cells were immunostained with the Tuj1 antibody (green). DNA was stained with DAPI (blue). Bar, 10 μ m. (C) The neurite-positive cells were counted. More than 100 cells were quantified. Data are shown as the means and SD ($n = 3$). (D) P19 cells were treated with RA for 24 h in the presence of thymidine and subjected to RT-PCR analysis with primers specific to *Tshz1* and β -actin. (E) P19 cells were treated with RA in the absence or presence of thymidine for up to 24 h. At the indicated time points, the cells were harvested and subjected to qPCR analysis of *Tshz1* expression. The values were normalized with *Gapdh*. Data are shown as the means and SD ($n = 3$). *, $P < 0.05$; **, $P < 0.01$; ***, $P < 0.001$. (F) P19 cells were treated with RA for 24 h in the presence of thymidine or RO3306 and subjected to qPCR analysis of *Tshz1* expression. *, $P < 0.05$; ***, $P < 0.001$.

under the control of the *Tshz1* promoter, which spans bp -1500 to $+500$ (Fig. 3A). Consistent with the quantitative PCR (qPCR) results, RA-induced activation of the reporter gene was significantly suppressed by thymidine treatment (Fig. 3A). These results suggest that the transcription of *Tshz1* is induced by RA, and such transcriptional activation partially depends on cell division. To define the minimal essential region of the *Tshz1* promoter that is responsible for RA-induced transcription, we generated reporter genes with truncated *Tshz1* promoter sequences. The results showed that

FIG 1 Legend (Continued)

with the Tuj1 antibody. DNA was stained with DAPI. Bar, 10 μ m. (E) The cells with primary neurites were counted, and results were statistically analyzed. More than 100 cells were quantified. Data are shown as the means and SD ($n = 3$). ***, $P < 0.001$.

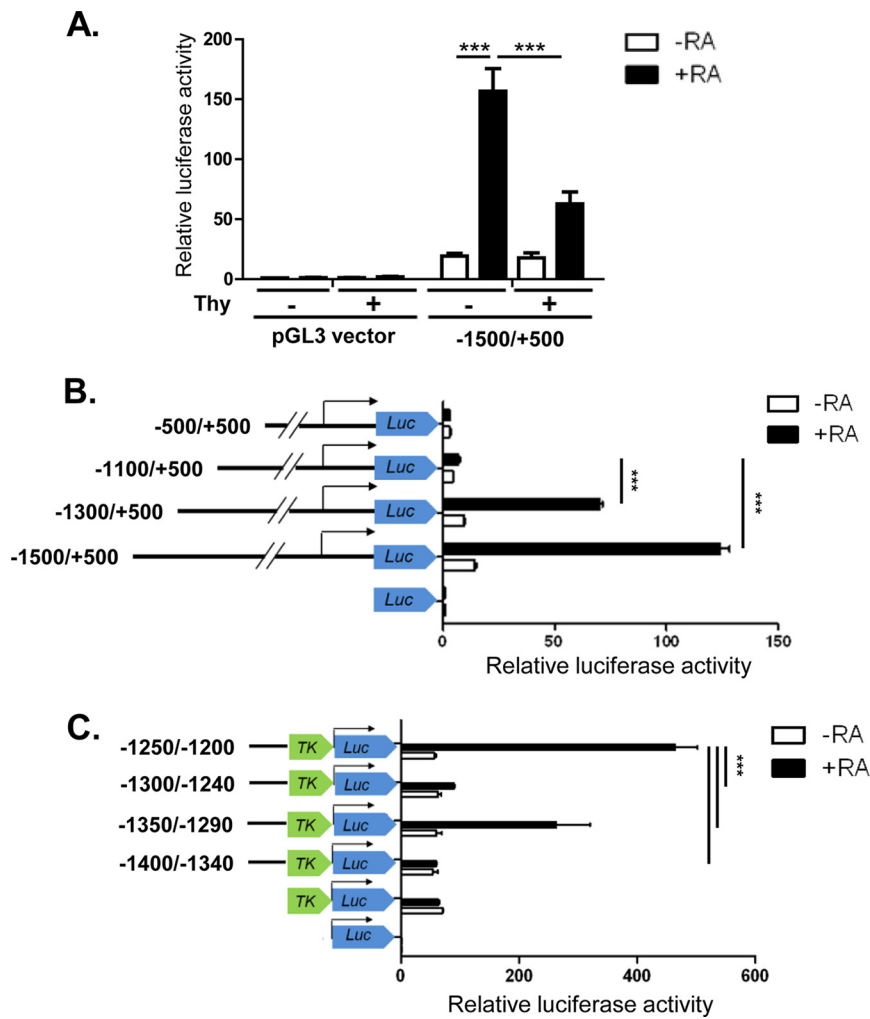


FIG 3 Promoter analysis of *Tshz1* for RA-induced activation. (A) The *luciferase* reporter gene was linked to the *Tshz1* promoter sequence (–1500/+500) and stably transfected into P19 cells. The cells were treated with RA for 24 h and subjected to reporter gene assays. Thymidine was added to block cell division. (B) Reporter gene assays were performed with fusion genes of different lengths of the *Tshz1* promoter sequence. (C) Different regions of the *Tshz1* promoter sequence were linked to the *TK-luciferase* reporter gene. The stable lines were treated with RA for 24 h and subjected to reporter gene assays. Data are shown as the means and SD ($n = 3$). ***, $P < 0.001$.

Tshz1^{–1500/+500} had a strong activity, while *Tshz1*^{–1100/+500} only had a minimal activity, suggesting that the –1500/–1100 region includes a *cis* element(s) for the RA-dependent activation of *Tshz1* transcription (Fig. 3B). Furthermore, we generated a fusion gene with 50-bp fragments within the –1400/–1200 region of the *Tshz1* promoter. The results showed that *Tshz1*^{–1250/–1200TK-Luc} generated the highest promoter activity, suggesting that an element important for RA-dependent activation may reside within the bp –1250 to –1200 region of the *Tshz1* promoter (Fig. 3C).

We performed electrophoretic mobility shift assays (EMSAs) to gain insight into which transcription factor binds to the –1250/–1200 fragment of the *Tshz1* promoter in an RA-dependent manner. The results showed a retarded band, which was detected in only the RA-treated group (Fig. 4A). The retarded band disappeared when the nuclear extracts were prepared from P19 cells treated with thymidine to block cell division (Fig. 4A). An EMSA was also performed with nuclear extracts from P19 cells treated with RA for various periods up to 24 h. The results showed that a specific retarded band appeared at 12 h post-RA treatment (Fig. 4B). This observation is consistent with the previous results in which the *Tshz1* transcript levels increased gradually after RA treatment (Fig. 2C).

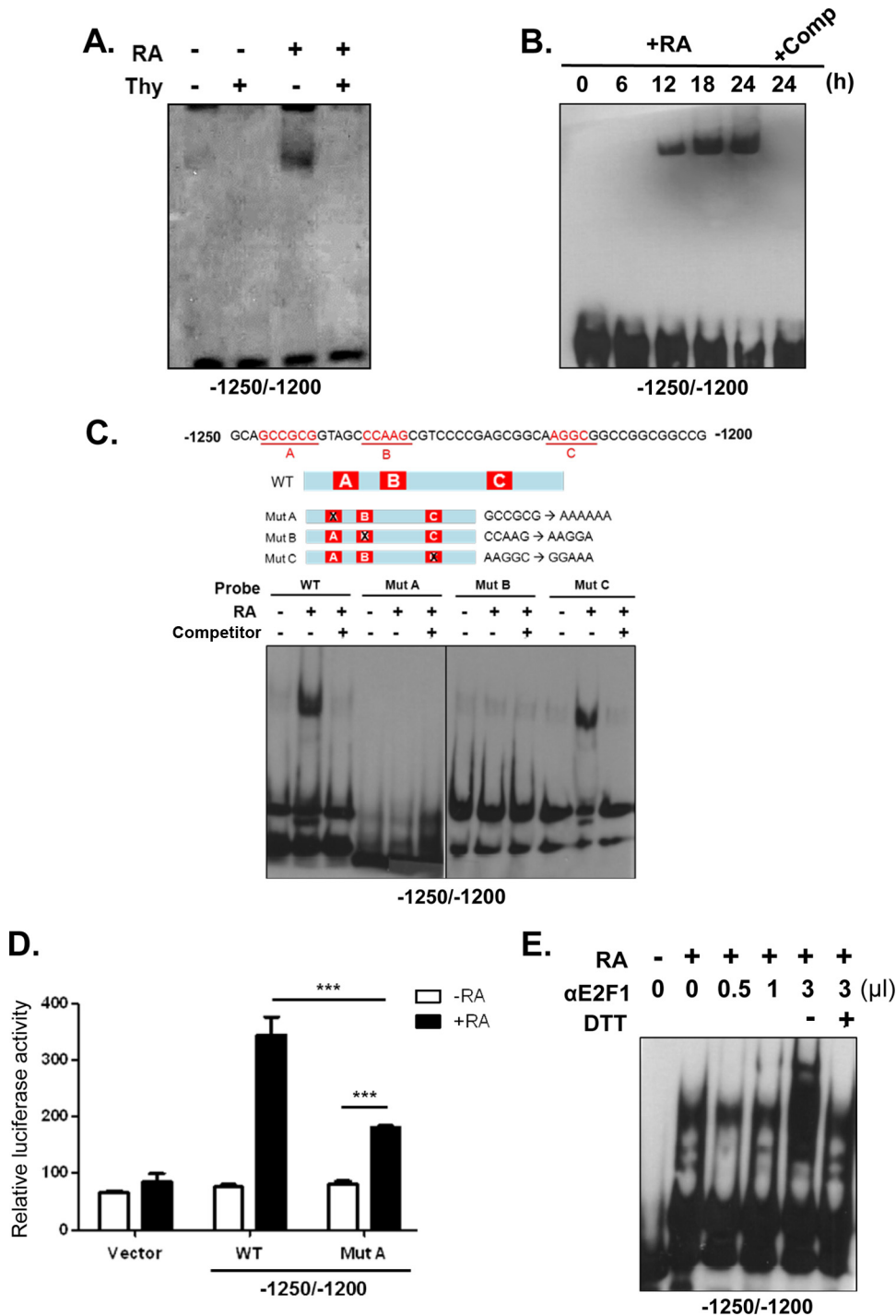


FIG 4 E2F1 binds to the *Tshz1* promoter. (A) The EMSA was performed using the -1250/-1200 region of the *Tshz1* promoter as a probe. Nuclear extracts were prepared from the RA-treated P19 cells that had been cultured in the presence of thymidine for 24 h. (B) The EMSA was performed with nuclear extracts from the P19 cells that had been cultured for the indicated time periods after RA treatment. Excess cold competitor was added in the final lane. (C) The EMSA was performed using the -1250/-1200 region of the *Tshz1* promoter as a probe. The reaction mixture included excess amounts of cold competitors with mutations at the regions indicated as A, B, and C in red boxes. (D) The wild-type and region A mutant of the -1250/-1200 *Tshz1* promoter were linked to the *TK-luciferase* reporter gene. The stable lines were treated with RA for 24 h and subjected to reporter gene assays. Data are shown as the means and SD ($n = 3$). $***, P < 0.001$. (E) The EMSA was performed using the *Tshz1* promoter -1250/-1200 fragment as a probe. Nuclear extracts were prepared from the RA-treated P19 cells. The indicated amounts of the E2F1 antibody were also added to the reaction mixture. DTT was added to disrupt antigen-antibody interactions.

A computational DNA sequence analysis using PROMO3.0 predicted 17 candidate transcription factors that can bind to the $-1250/-1200$ fragment of the mouse *Tshz1* promoter (16). Binding sites of the transcription factors were grouped according to three common regions (regions A, B, and C [Fig. 4C]). We performed EMSA analyses with probes that had mutations at each common region. The mutant probes at regions A and B failed to produce a retarded band, but the region C mutant probe had a retarded band. Thus, sequences within regions A and B, but not region C, are important for binding a transcription factor(s) during RA induction (Fig. 4C). The *Tshz1* promoter $-1250/-1200$ containing a mutation within region A was tested for promoter activity, and the result showed reduced activity compared to that of the wild-type promoter (Fig. 4D). These results suggest that region A is an important binding site for a transcription factor whose sequence-specific binding activity is induced by RA treatment.

E2F1 as a mediator for RA-induced *Tshz1* transcription. One of the transcription factors predicted to bind to region A of the *Tshz1* promoter is E2F1, which is well known to be important for progression through the G₁/S transition (17). In addition to the canonical role of E2F1 as a cell cycle regulator, its functional diversity has been strongly suggested during the cell fate decisions of stem and progenitor cells (18). In fact, E2F family members are known to regulate genes related to lineage choices during adipogenesis, myogenesis, pancreatic differentiation, and neurogenesis (19–23). With this in mind, we performed a supershift EMSA with the E2F1 antibody. The results showed that the addition of an E2F1 antibody supershifted the retarded band when the $-1250/-1200$ fragment was used a probe (Fig. 4E). The supershifted band disappeared after dithiothreitol (DTT) treatment for the disruption of antigen-antibody interactions (Fig. 4E). These results suggest that E2F1 is a candidate transcription factor that binds to the region A of the *Tshz1* promoter.

We performed reporter gene assays to determine whether E2F1 can activate *Tshz1* transcription in an RA-dependent manner. P19 cells were transfected with an E2F1-expressing vector and treated with RA. Immunoblot analysis confirmed the abundant expression of ectopic E2F1 (Fig. 5A). The luciferase activity of *Tshz1* ^{$-1250/-1200$ -TK-luc} was enhanced in lysates from E2F1-overexpressing cells (Fig. 5B). We did not observe such enhancement in the region A-mutated reporter gene (*Tshz1* ^{$-1250/-1200$ MutA-TK-luc}) (Fig. 5B). We also performed promoter activity assays with P19 cells in which endogenous E2F1 was depleted by specific *E2F1* small interfering RNAs (siRNAs) (Fig. 5C). The results showed that the luciferase activity of *Tshz1* ^{$-1250/-1200$ -TK-luc} was reduced in lysates from E2F1-depleted P19 cells (Fig. 5D). Such a reduction was not observed with the region A-mutated reporter gene (Fig. 5D). These results suggest that E2F1 mediates the RA-induced activation of *Tshz1* transcription.

The requirement of cell division for the E2F1-dependent activation of *Tshz1* transcription was examined by reporter gene assays. RA-dependent activation of the *Tshz1* promoter was enhanced by overexpression of E2F1, but such activation was nullified by the thymidine treatment (Fig. 5E). Furthermore, RA-dependent activation was diminished by depletion of E2F1 and remained reduced with thymidine treatment (Fig. 5F). These results imply that the enhancing effect of E2F1 on *Tshz1* promoter activity requires cell division during RA-induced differentiation in P19 cells.

If E2F1 is an upstream regulator of *Tshz1* transcription, E2F1 might directly bind to the *Tshz1* gene. We performed chromatin immunoprecipitation (ChIP) assays to determine whether E2F1 directly binds to the *Tshz1* promoter *in vivo*. Nuclear extracts from P19 cells were immunoprecipitated with the E2F1 antibody and PCR amplified with primers specific to *Tshz1*. The *Tshz1* gene fragments were coimmunoprecipitated with E2F1 (Fig. 6A). Furthermore, the amount of coimmunoprecipitated *Tshz1* gene fragments increased after RA treatment (Fig. 6A). However, the specific band was not observed with HeLa cell lysates even with RA treatment (Fig. 6A). These results are consistent with the hypothesis that E2F1 mediates the RA-induced activation of *Tshz1* transcription during the neurogenesis of P19 cells.

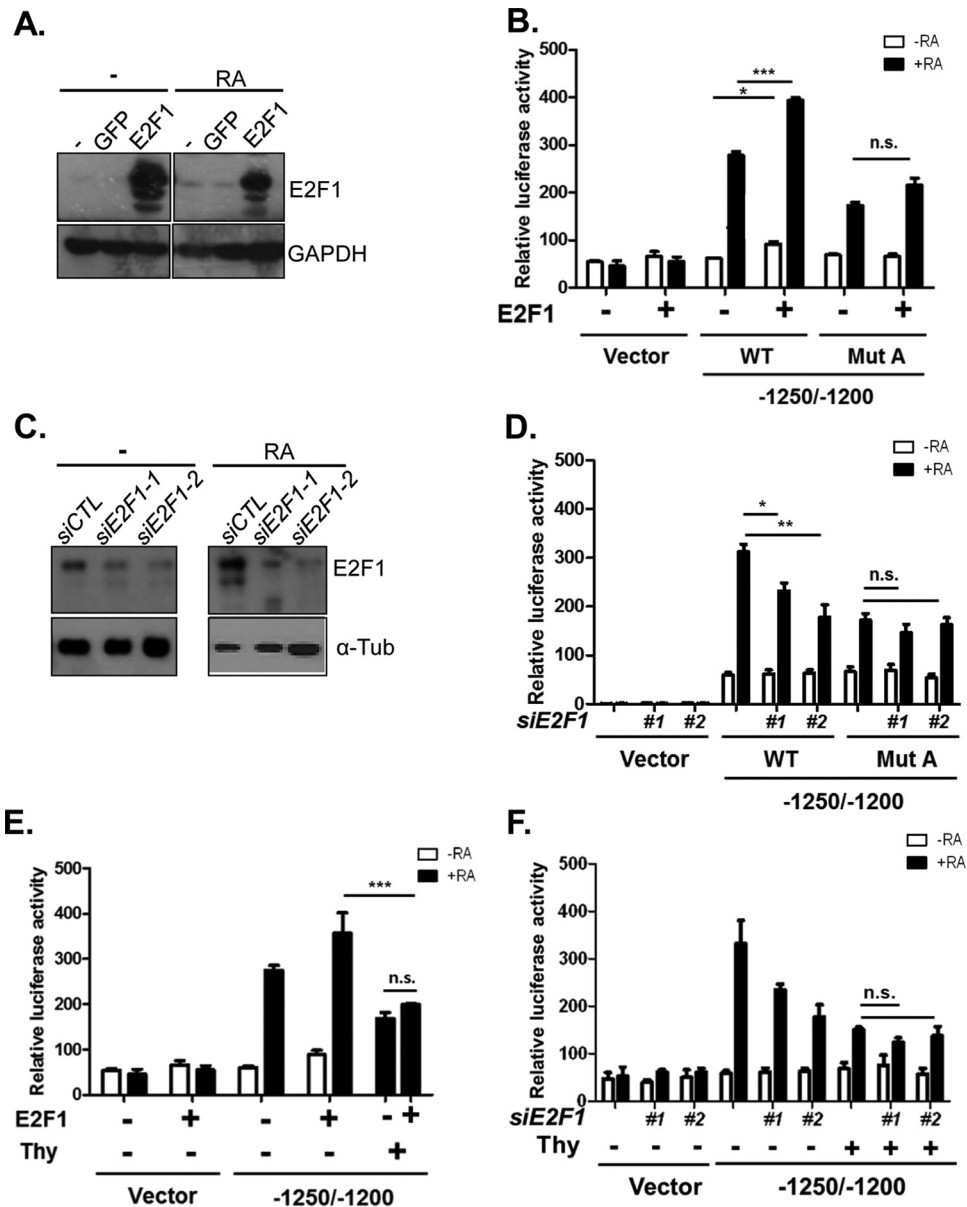


FIG 5 E2F1-dependent activation of *Tshz1* transcription. (A, C) Immunoblot analyses were performed with P19 cells that had been transiently transfected with an E2F1-expressing construct (A) and siRNAs specific to E2F1 (C). (B, D to F) E2F1 expression vector (B) and siRNAs specific to E2F1 (D) were transfected into P19 cells that had been stably transfected with the wild-type and A-type mutant *Tshz1*^{-1250/-1200}-TK-luciferase constructs. Thymidine treatment was applied to the E2F1-overexpressing (E) and E2F1-depleted (F) P19 cells. Twenty-four hours after the RA treatment, the cells were subjected to reporter gene assays. Data are shown as the means and SD (*n* = 3). *, *P* < 0.05; **, *P* < 0.01; ***, *P* < 0.001; n.s., nonsignificant.

E2F1 is known to interact with retinoblastoma protein (Rb) during the G₁ phase (24–26). Cyclin D-dependent kinases cumulatively phosphorylate Rb during the G₁ phase and eventually allow the release of E2F1 from hyperphosphorylated Rb for S phase progression (27, 28). We asked whether the E2F1 binding to the *Tshz1* promoter depends on a specific cell cycle stage. To test the hypothesis, we arrested the P19 cells at the G₁/S phase and synchronously released them to the S phase (see Fig. S1A in the supplemental material). A group of P19 cells were treated with RA at the same time. We prepared cell lysates at the indicated time points and subjected them to immunoblot and ChIP-qPCR analyses. Immunoblot analysis revealed that Rb was hyperphosphorylated during the S phase irrespective of RA treatment (Fig. S1B and C). We observed

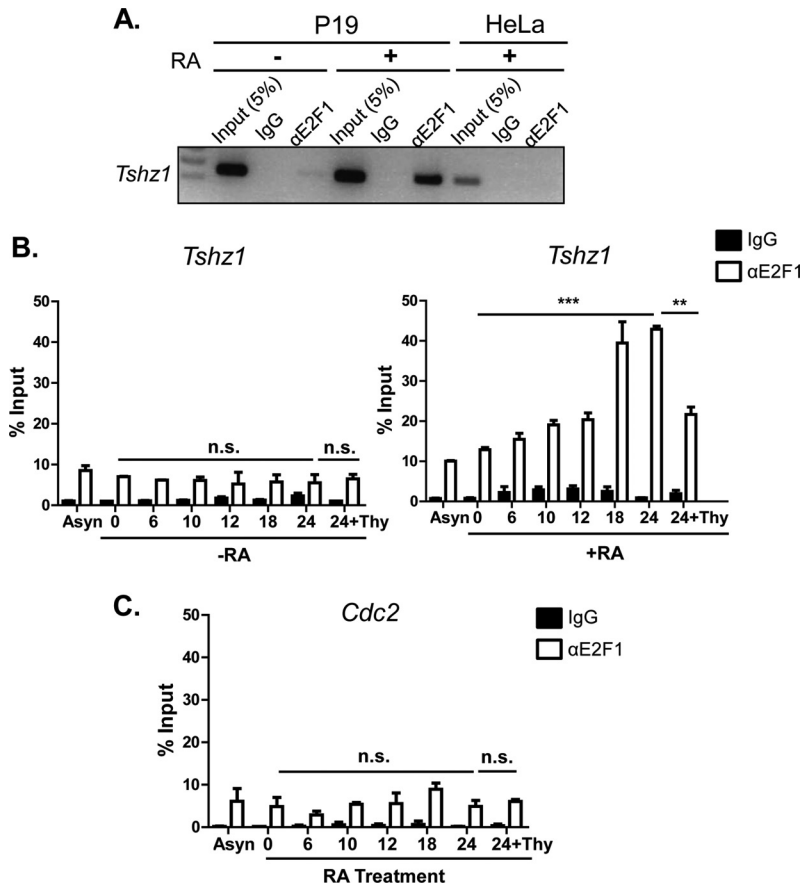


FIG 6 Direct binding of E2F1 to the *Tshz1* promoter. Nuclear extracts were prepared from P19 and HeLa cells that had been treated with RA for 24 h. (A) ChIP-PCR analysis was performed with the E2F1 antibody and primers specific to the coding sequence of *Tshz1*. (B, C) P19 cells were arrested at the G₁/S phase and synchronously released to the S phase. Simultaneously, the cells were treated with RA and harvested at the indicated time points. ChIP-qPCR analysis was performed with the E2F1 antibody. The target region was amplified using primers specific to the promoter regions of *Tshz1* (B) and *Cdc2* (C).

constant expression of other Rb family proteins, such as p107 and p130, in the synchronized population (Fig. S1C). The ChIP-qPCR results showed little binding of Rb family proteins to the *Tshz1* promoter throughout RA treatment (Fig. S1D to F). Meanwhile, the E2F1 binding activity to the *Tshz1* promoter significantly increased at 18 h after RA treatment (Fig. 6B). However, we did not observe any increase in E2F1 binding to the *Tshz1* promoter in the S phase populations (Fig. 6B). Furthermore, no S phase-specific binding of E2F1 was observed in the synchronous P19 populations without RA (Fig. 6B). We also performed ChIP assays for E2F1 on the *Cdc2* promoter, which is a known target of E2F1 (29). The E2F1 binding activity to the *Cdc2* promoter fluctuated within an error range (Fig. 6C) and did not change after RA treatment, while E2F1 binding activity to *Tshz1* was significantly enhanced by RA treatment (Fig. 6B). These results revealed that *Tshz1* is a specific target of E2F1 for the neuronal differentiation of P19 cells. Furthermore, these results strongly support that E2F1 mediates the RA activation of *Tshz1* transcription in a cell division-dependent manner.

We determined the effects of various cellular levels of E2F1 on *Tshz1* transcription during the RA-induced differentiation of P19 cells. E2F1 overexpression significantly enhanced the RA-dependent induction of the *Tshz1* transcript levels (Fig. 7A). We also examined the effects of E2F1 depletion on *Tshz1* expression. As expected, the *Tshz1* transcript levels were reduced by 30% compared to those in the *siCTL* group when endogenous E2F1 was depleted (Fig. 7B). These results indicate that E2F1 is a transcription factor that mediates the RA-dependent transcription of *Tshz1*.

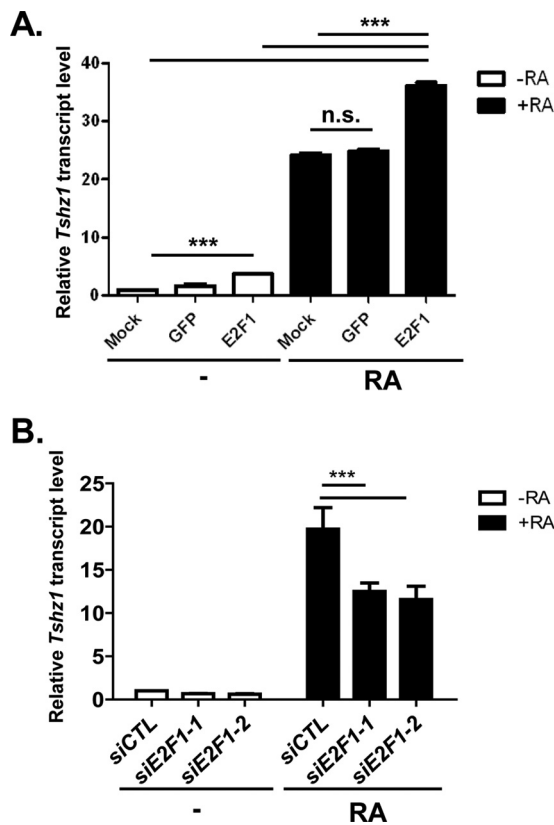


FIG 7 E2F1 is a transcriptional activator of *Tshz1*. E2F1-expressing (A) and E2F1-depleted (B) P19 cells were treated with RA for 24 h and subjected to qRT-PCR analysis to determine endogenous *Tshz1* mRNA levels. Data are shown as the means and SD ($n = 3$). ***, $P < 0.001$; n.s., nonsignificant.

Effect of E2F1 depletion on the neuronal differentiation of P19 cells. We determined the importance of E2F1 activity during the neuronal differentiation of P19 cells. Immunoblot analysis revealed that RA treatment induced a significant increase in cellular E2F1 levels in P19 cells (Fig. 8A). However, cell proliferation slowed down, as indicated by an increase in p27 and a decrease in cyclin B1 protein levels (Fig. 8A). The transfection of siRNAs specific to *E2F1* reduced cellular E2F1 levels irrespective of RA treatment (Fig. 8B), and *Tshz1* transcript levels were significantly reduced in the E2F1-depleted cells (Fig. 8C). The number of cells with neurites was significantly reduced in the P19 cells depleted of *Tshz1* or E2F1 (Fig. 8D and E). Codepletion of both *Tshz1* and E2F1 also reduced neuronal differentiation to levels comparable to those after individual depletions (Fig. 8F). These results suggest that *Tshz1* and E2F1 function in the same pathway in terms of neuronal differentiation.

DISCUSSION

It is known that cell division can be part of the regulatory processes for stem cell differentiation. In this work, we used P19 embryonic carcinoma cells as a model to determine the involvement of cell division during neuronal differentiation. We investigated the induction mechanisms of *Tshz1* expression to elucidate the mechanisms underlying the cell division-dependent regulation of neuronal differentiation. A series of experiments was used to identify E2F1 as a cell division-dependent induction factor for *Tshz1* transcription. Based on our results, we propose that E2F1 mediates the neuronal differentiation of P19 cells in a cell division-dependent manner (Fig. 9).

E2F1 is a transcription factor that activates a group of genes required for S phase progression during the cell cycle. The canonical targets of E2F1 include cell cycle regulators, enzymes for nucleotide synthesis, DNA replication, and DNA repair, and proteins involved in chromosome organization and segregation (30–32). It is also

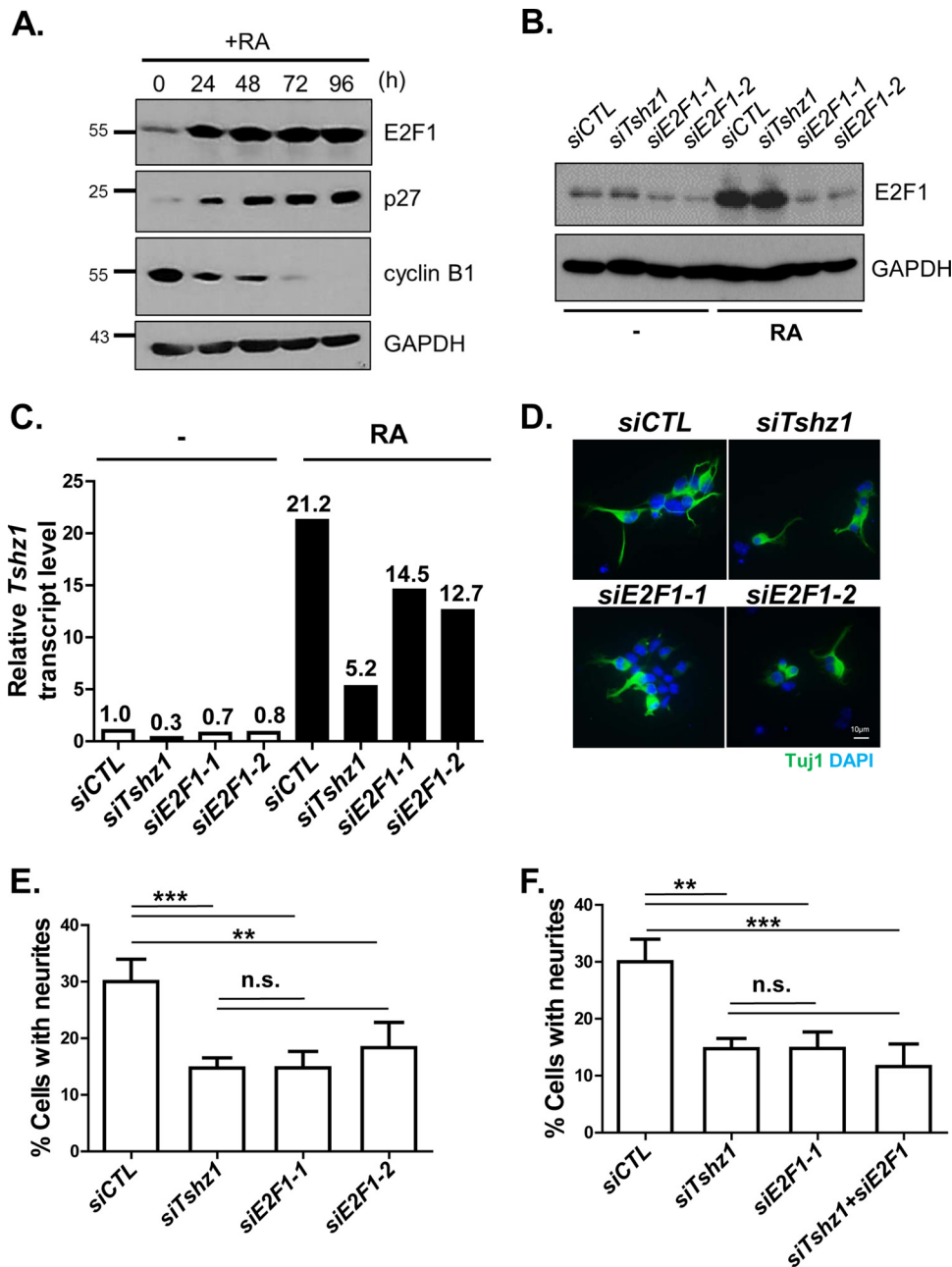


FIG 8 Effects of E2F1 depletion on the neuronal differentiation of P19 cells. (A) Immunoblot analyses were performed with P19 cells that had been harvested at the indicated time points after RA treatment with antibodies specific to E2F1, p27, cyclin B1, and GAPDH. (B) Immunoblot analysis of E2F1 was performed in P19 cells that had been transfected with siRNAs specific to *Tshz1* and *E2F1*. (C) The endogenous *Tshz1* transcript level was quantified by qRT-PCR. (D) *Tshz1*- or E2F1-depleted P19 cells were cultured for neuronal differentiation and immunostained with the Tuj1 antibody (green). DNA was stained with DAPI (blue). Bar, 10 μ m. (E, F) The neurite-positive cells were counted in *Tshz1*- and/or E2F1-depleted cells. More than 100 cells were quantified. Data are shown as the means and SD ($n = 3$). ***, $P < 0.001$; **, $P < 0.01$; n.s., nonsignificant.

known that the same E2F1 activates a different set of genes for cell fate determination and differentiation (18). In fact, *E2F1* knockout mice have reduced populations of stem and progenitor cells in postnatal brains (33). Expanded noncanonical functions of E2F1 are supported by a recent ChIP-seq-based study in which a new class of E2F1-target genes were identified that are not cell cycle-related. The targets were related to diverse biological processes, including metabolic pathways and cellular responses to stimuli (34). The multiple functions of E2F1 are linked to the biphasic bindings of E2F1 with

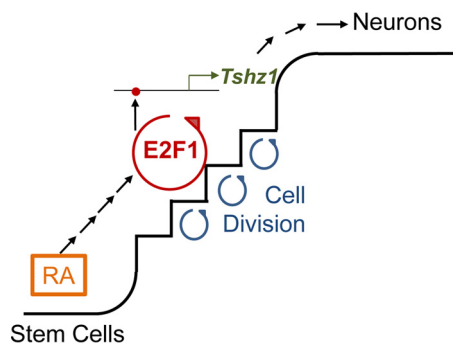


FIG 9 Model. RA initiates the neuronal differentiation of P19 cells. Expression of *Tshz1*, an upstream transcription factor for neuronal differentiation, is induced by RA. E2F1 mediates the transcriptional activation of *Tshz1* in a cell division-dependent manner.

pocket proteins and interaction partners (18, 35). E2F1 also recruits histone acetyltransferase to local chromatin for epigenetic regulation (36).

A few mechanisms have been proposed for the functions of E2F family proteins in diverse differentiation processes. First, E2F plays a role in the expansion of a specific stage of progenitor cells during differentiation. In the case of early pancreas development, E2F1 activates *neurogenin-3* transcription and induces the expansion of a specific lineage of beta cell progenitors (21). Second, E2F members directly regulate the expression of a group of genes required for the execution of a specific differentiation event. For example, E2F3 regulates *neogenin*, a gene encoding a receptor for cell migration and axon guidance in mouse forebrain (22). The study showed that pRB/E2F-dependent regulation of *neogenin* expression is required for neural precursor migration, which is important for brain development (22). Another example is E2F1 regulation of lipid synthesis. E2F1 directly binds to the promoters of key lipogenic genes, including *fatty acid synthase*, and increases lipogenesis (34). E2F1 participation in lipid synthesis might be linked to the synthesis of new membranes for cell size expansion (34).

In this study, we confirmed E2F1 as a direct mediator of neuronal differentiation since it regulates *Tshz1*, an upstream transcription factor for neuronal differentiation (37, 38). E2F1 does not activate *Tshz1* transcription in a cell cycle stage-specific manner, as shown by the ChIP-qPCR analyses (Fig. 6B). Rather, activation of *Tshz1* transcription might be closely linked to the augmentation of cellular E2F1 levels by RA treatment (Fig. 8A). E2F1 activity should be selective since *Cdc2*, a known target of E2F1, was not activated along with *Tshz1* during the neuronal differentiation of P19 cells (Fig. 6C). The specificity of the target genes may be determined by the interaction of a protein binding to E2F1 during neuronal differentiation. We will now investigate the binding protein(s) of E2F1 during the neuronal differentiation of P19 cells.

MATERIALS AND METHODS

Antibodies and primers. The antibodies against Tuj1 (MMS-435p-100; Covance), p27 (ab7961; Abcam), E2F1 (sc-251; Santa Cruz Biotechnology), green fluorescent protein (GFP; sc-9996; Santa Cruz Biotechnology), Flag (F3165; Sigma-Aldrich), GAPDH (glyceraldehyde-3-phosphate dehydrogenase; AM4300; Ambion), pRb (554136; BD Pharmingen), p107 (SC-250; Santa Cruz), p130 (SC-374521; Santa Cruz), cyclin B1 (sc-254; Santa Cruz Biotechnology), and α -tubulin (ab18251; Abcam) were commercially purchased. The secondary antibody conjugated with fluorescent dye (Alexa Fluor 488; Life Technologies) was also purchased. The mouse and rabbit IgG-horseradish peroxidase (HRP) antibodies were purchased from Sigma and Millipore, respectively. For depletion of *E2F1* and *Tshz1*, *siE2F1-1* (5'-CGC UAU GAA ACC UCA CUA ATT-3'), *siE2F1-2* (5'-GUG GAU UCU UCA GAG ACA UTT-3'), and *siTshz1* (5'-CCC AGA UAC UCA AGU GCA UTT-3') were used. A scrambled siRNA sequence (*siCTL*; 5'-UUC UCC GAA CGU GUC ACG UTT-3') was used as a control. RNAiMAX (13778-075; Invitrogen) was used for siRNA transfection according to the manufacturer's protocol.

For the RT-PCR and qPCR analyses, we used primer sets of *Tshz1* (forward, 5' GCT GGC CCA TTT CAA AAG CTC 3'; reverse, 5' ATC CAA TGC TAG GCT AGA CCA 3'), *Hmbs* (forward, 5' ACT CTG CTT CGC TGC ATT G 3'; reverse, 5' AGT TGC CCA TCT TTC ATC ACT G 3'), β -actin (forward, 5' CAT CAT GAA GTG TGA

CGT TG 3'; reverse, 5' ATG ATC TTG ATC TTC ATG GT 3'), and *GAPDH* (forward, 5' CTG CCT TGG AGA AGC TCA GT 3'; reverse, 5' CAC CAA GTC GAT CAG ACC AA 3').

For the ChIP-qPCR analysis, we used primer sets targeting the *Tshz1* coding region (forward, 5' GCT GGC CCA TTT CAA AAG CTC 3'; reverse, 5' ATC CAA TGC TAG GCT AGA CCA 3'), the *Tshz1* promoter region (forward, 5' ACC CCA GGA TCC CTG CCC 3'; reverse, 5' CGC TCG GGG TTG ATT CGT ACC A 3'), *cdc2* (forward, 5' ACA GAG CTC AAG AGT CAG TTG GC 3'; reverse, 5' CGC CAA TCC GAT TGC ACG TAG A3').

Cell culture, drug treatment, and neuronal differentiation. P19 embryonic carcinoma cells were cultured in Dulbecco's modified Eagle medium (DMEM; LM001-05; Welgene) supplemented with 10% fetal bovine serum (FBS), 5 μ g/ml ANT-MPT (InvivoGen), and antibiotics (S101-01; Welgene).

For the cell cycle block experiments, the cells were first synchronized at G₁ phase using a single or double thymidine block. The single thymidine block was performed with 2 mM thymidine (T9250; Sigma) for 12 h. The double thymidine block was performed with 2 mM thymidine (T9250; Sigma) for 12 h, followed by 6 h of release into thymidine-free medium and thymine treatment for another 12 h. Upon thymidine release, the cells were treated with cell cycle-blocking drugs. For G₂ arrest, the cells were treated with RO3306 (10 μ M) for 12 h.

To generate polyclonal stable cell lines, 4 \times 10⁴ P19 cells were seeded on a 24-well plate. The next day, 1 μ g of plasmid DNA was transfected using Lipofectamine 3000 (L3000001; Invitrogen) according to the manufacturer's instructions. One day after the transfection, the cells were transferred to a 100-mm dish and subjected to G418 selection for 1 to 2 weeks.

To differentiate P19 cells to neurons, the conventional method was performed essentially according to the previous report (39). Briefly, P19 cells (10⁵ cells/ml) were cultured in suspension in a petri dish in DMEM containing 10% FBS that was treated with 1 μ M all *trans*-retinoic acid (R2656; Sigma) to allow for the EB formation for at least 2 days (or as otherwise indicated in the figure legend). The EBs were then trypsinized and replated into a poly-L-lysine-coated tissue culture dish and cultured in FBS-free B27-supplemented DMEM (catalog number 17504044; Gibco) for up to 4 days.

Immunocytochemistry analysis. P19 cells were seeded on cover glass and were fixed with cold methanol for 10 min and washed three times with ice-cold phosphate-buffered saline (PBS). After incubation in PBST (0.1% Triton X-100 in PBS) for 10 min, the cells were blocked with blocking solution (3% bovine serum albumin in 0.3% Triton X-100 in PBS) for 30 min. Then, cells were incubated with primary antibodies at room temperature diluted in blocking solution for 1 h. Cells were washed three times with PBST and incubated with fluorescent dye-conjugated secondary antibodies diluted in blocking solution for 30 min. Afterwards, cells were washed twice with PBST, incubated with 4,6-diamidino-2-phenylindole (DAPI) solution for 3 min, and washed twice with PBST. The cover glasses were mounted on a slide glass with ProLong Gold antifade reagent (P36930; Life Technologies). Images were acquired from fluorescence microscopes equipped with digital cameras (Olympus IX51 equipped with QImaging QICAM Fast 1394 or Olympus IX81 equipped with ANDOR iXonEM+) and processed in ImagePro 5.0 (Media Cybernetics).

Neurite outgrowth assay. Typically, pictures of 30 to 50 neurons from three separate coverslips from each experiment were taken using a fluorescence microscope (Leica DMI6000B). Representative cells with strong TuJ1 immunoreactivity labeled neurite (axonal and dendritic) processes were analyzed. Neurites with lengths that were at least twice the diameter of the cell body were considered neurite-positive cells. Neurite lengths from the cell body and cell body diameter were traced and measured using NeuronJ (ImageJ) software, and the data were compiled and analyzed using Prism (GraphPad).

Immunoblot analysis. Cells were lysed on ice for 20 min with radioimmunoprecipitation assay (RIPA) lysis buffer (150 mM NaCl, 1% Triton X-100, 0.5% sodium deoxycholate, 0.1% SDS, 50 mM Tris-HCl at pH 8.0, 10 mM NaF, 1 mM Na₃VO₄, 1 mM EDTA, and 1 mM EGTA) containing a protease inhibitor cocktail (P8340; Sigma-Aldrich) and centrifuged at 12,000 rpm for 15 min at 4°C. The supernatants were mixed with 5 \times SDS sample buffer (250 mM Tris-HCl at pH 6.8, 10% SDS, 50% glycerol, and 0.02% bromophenol blue) and 10 mM DTT (0281-25G; Amresco). Mixtures were boiled for 7 min. The cell lysates (20 to 30 μ g protein) were loaded onto an SDS-polyacrylamide gel and transferred onto nitrocellulose membranes (GE Healthcare). For the analysis of Rb family proteins, 4 to 6% SDS-polyacrylamide gel was used. The membranes were blocked with blocking solution (5% nonfat milk in 0.1% Tween 20 in Tris-buffered saline [TBS]) for 1 h at room temperature and incubated with primary antibodies diluted in blocking solution overnight at 4°C. In the case of Rb family proteins, 5% bovine serum albumin (BSA) was used as blocking solution. Then, membranes were washed for 15 min four times with TBST (0.1% Tween 20 in TBS) and incubated with HRP-conjugated secondary antibodies in blocking solution for 45 min at room temperature and washed again with TBST. To detect the signals of secondary antibodies, an enhanced chemiluminescence (ECL) solution (LF-QC0101; ABfrontier) and X-ray films (CP-BU NEW; Agfa) were used.

RT-PCR and qPCR. Total RNAs were extracted using TRIzol (Invitrogen), and reverse transcription was performed from 2 μ g total RNAs using RnaUsScript RTase (LeGene) according to the manufacturer's instructions. Then, the samples were first subjected to RT-PCR using 1 μ l of reverse transcription product with the 2 \times HOT PCR mastermix (catalog number MP00505; Doctor Protein) according to the manufacturer's instructions. Briefly, a total of 20 μ l reaction mixture was prepared containing 1 μ l of reverse transcription product, 5 pmol of each forward and reverse PCR primer, and the 2 \times *Taq* polymerase mixture provided by the manufacturer. Then, the mixture was subjected to incubation at 95°C for 2 min followed by 30 cycles of 95°C for 30 s, 55°C for 30 s, and 72°C for 30 s. Ten microliters of the amplified reaction mixture was electrophoresed on a 1.5% agarose gel followed by staining with ethidium bromide and imaging for PCR product. For qPCR, 1 μ l of reverse transcription product, 10 pmol of each forward and reverse PCR primer, and SYBR TOPreal qPCR 2 \times PreMix (Enzynomics) were used. The abundance of

mRNA was determined by an ABI prism 7500 system. The quantity of mRNA was calculated using the $\Delta\Delta C_T$ method (where C_T is threshold cycle), and *beta-actin*, *Gapdh*, and *Hmbs* were used as control.

Luciferase assay. A promoter reporter construct containing the indicated regions relative to the transcription start site of the *Tshz1* promoter was cloned from P19 cells' genomic DNA and inserted upstream of the firefly luciferase reporter in the *pGL3-Basic* vector (Promega). To generate a stable cell line of luciferase reporter, a neomycin (kanamycin)-expressing sequence was inserted into the firefly luciferase reporter vector. Twenty-four hours after transfection, P19 cells were subjected to G418 selection for 1 week. Then, polyclonal cell lines were subjected to luciferase assays using a microplate luminometer (DE/LB 96V; Berthold Technologies). For construction of *Tshz1* mutants, site-directed mutagenesis was performed. One day after seeding 2×10^4 stable cells in a 24-well plate, cells were treated with the indicated drugs with or without RA for 24 h. Then, cells were lysed and subjected to luciferase assay. After cell lysis, the luciferase assay was performed within 2 h. Luciferase outputs were normalized by total protein amount measured via the Bradford assay. All values were calculated as relative to *pGL3* vector.

EMSA. The oligonucleotides were first biotinylated and annealed, using the biotin 3' end DNA labeling kit (89818; Pierce). Nuclear extracts were prepared from P19 cells using nuclear extraction buffer. The binding reactions were performed on ice for 20 min with nuclear extract and 20 fmol of biotin-labeled DNA in a final volume of 20 μ l, containing 2 μ l of $10\times$ binding buffer (100 mM Tris, 500 mM KCl, 10 mM DTT; pH 7.5) and 1 μ l of poly(dI-dC). For supershift assays, 1 to 3 μ g of E2F1 antibody (Santa Cruz Biotechnology) was added to the reaction mixture described above, followed by incubation on ice for 15 min prior to the addition of the labeled oligonucleotide probe. A double-stranded mutated oligonucleotide and unlabeled double-stranded oligonucleotides were used as competitors (400 fmol) to examine the specificity of DNA binding. For all the supershift assays, DTT-free buffers were used. The resultant DNA-protein complex was resolved from free oligonucleotide in a 6% native polyacrylamide gel in Tris borate-EDTA buffer and transferred to nylon membranes (Bio-Rad). The membranes were cross-linked by UV radiation using Gel-doc (Bio-Rad). Biotin signal detection was performed using the chemiluminescent nucleic acid detection module (89880; Thermo Fisher Scientific) in accordance with the manufacturer's instructions.

Chromatin immunoprecipitation assay. P19 cells (or HeLa cells) were cross-linked with 1% formaldehyde for 10 min at room temperature. After glycine quenching to a final concentration of 0.2 M for 10 min at room temperature, the cell pellets were lysed in buffer containing 50 mM Tris-HCl (pH 8.1), 10 mM EDTA, and 1% SDS, supplemented with complete protease inhibitor cocktail (Roche), and sonicated. Chromatin extracts containing DNA fragments with an average of 250 bp were then diluted 10 times with dilution buffer containing 1% Triton X-100, 2 mM EDTA, 150 mM NaCl, and 20 mM Tris-HCl (pH 8.1) with complete protease inhibitor cocktail, precleared with protein A/G-Sepharose (17-0780-01; GE Healthcare Life Sciences) and subjected to immunoprecipitations overnight at 4°C by incubating with 3 μ g of E2F1 antibody (sc-251; Santa Cruz Biotechnology) and mouse IgG as a negative control. Immunocomplexes were captured by incubating 45 μ l of protein A/G-Sepharose for 2 h at 4°C. Beads were washed with low-salt wash buffer (0.1% SDS, 1% Triton X-100, 2 mM EDTA, 20 mM Tris-HCl [pH 8.1], 150 mM NaCl), high-salt wash buffer (0.1% SDS, 1% Triton X-100, 2 mM EDTA, 20 mM Tris-HCl [pH 8.1], 500 mM NaCl), buffer III (0.25 M LiCl, 1% NP-40, 1% deoxycholate, 10 mM Tris-HCl [pH 8.1], 1 mM EDTA), and Tris-EDTA (TE) buffer (10 mM Tris-HCl [pH 8.0], 0.5 M EDTA) and eluted in elution buffer (1% SDS, 0.1 M NaHCO₃). The supernatant was incubated overnight at 65°C to reverse-cross-link and then digested with RNase A for 2 h at 37°C and proteinase K for 2 h at 55°C. ChIP samples as well as 1% of DNA extract from soluble chromatin that was used as input DNA were then purified for qPCR analysis using the primers indicated. Enrichment relative to input values were calculated using the percent input method.

FACS analysis. Samples were collected over indicated time points and fixed in 70% ethanol overnight. For cell cycle analysis, fixed cells were treated with RNase for 20 min before addition of 5 μ g/ml propidium iodide (PI) and analyzed by fluorescence-activated cell sorter (FACS; BD Biosciences FACSCalibur).

Statistical analysis. All experiments were performed independently at least three times. Values are expressed as means \pm standard deviations (SD). *P* values were analyzed using the two-tailed unpaired *t* test and one-way analysis of variance (ANOVA). *P* values of <0.05 were considered statistically significant.

SUPPLEMENTAL MATERIAL

Supplemental material for this article may be found at <https://doi.org/10.1128/MCB.00217-18>.

SUPPLEMENTAL FILE 1, PDF file, 0.3 MB.

ACKNOWLEDGMENT

We thank Jae Sang Kim (Ewha Womens University), Deog Su Hwang (Seoul National University), and Jae Bum Kim (Seoul National University) for generously providing us with the P19 cell line and antibodies.

This research was supported by the Basic Science Research Program through the National Research Foundation of Korea funded by the Ministry (NRF2014R1A4A1005259 and 2016R1A2B4009418).

REFERENCES

- Guo L, Li X, Tang QQ. 2015. Transcriptional regulation of adipocyte differentiation: a central role for CCAAT/enhancer-binding protein (C/EBP) beta. *J Biol Chem* 290:755–761. <https://doi.org/10.1074/jbc.R114.619957>.
- Wu Z, Xie Y, Bucher NL, Farmer SR. 1995. Conditional ectopic expression of C/EBP beta in NIH-3T3 cells induces PPAR gamma and stimulates adipogenesis. *Genes Dev* 9:2350–2363. <https://doi.org/10.1101/gad.9.19.2350>.
- Cao Z, Umek RM, McKnight SL. 1991. Regulated expression of three C/EBP isoforms during adipose conversion of 3T3-L1 cells. *Genes Dev* 5:1538–1552. <https://doi.org/10.1101/gad.5.9.1538>.
- Li X, Kim JW, Gronborg M, Urlaub H, Lane MD, Tang QQ. 2007. Role of cdk2 in the sequential phosphorylation/activation of C/EBPbeta during adipocyte differentiation. *Proc Natl Acad Sci U S A* 104:11597–11602. <https://doi.org/10.1073/pnas.0703771104>.
- Soufi A, Dalton S. 2016. Cycling through developmental decisions: how cell cycle dynamics control pluripotency, differentiation and reprogramming. *Development* 143:4301–4311. <https://doi.org/10.1242/dev.142075>.
- Pauklin S, Vallier L. 2013. The cell-cycle state of stem cells determines cell fate propensity. *Cell* 155:135–147. <https://doi.org/10.1016/j.cell.2013.08.031>.
- Hardwick LJ, Ali FR, Azzarelli R, Philpott A. 2015. Cell cycle regulation of proliferation versus differentiation in the central nervous system. *Cell Tissue Res* 359:187–200. <https://doi.org/10.1007/s00441-014-1895-8>.
- Pauklin S, Madrigal P, Bertero A, Vallier L. 2016. Initiation of stem cell differentiation involves cell cycle-dependent regulation of developmental genes by Cyclin D. *Genes Dev* 30:421–433. <https://doi.org/10.1101/gad.271452.115>.
- Jones-Villeneuve EM, McBurney MW, Rogers KA, Kalnins VI. 1982. Retinoic acid induces embryonal carcinoma cells to differentiate into neurons and glial cells. *J Cell Biol* 94:253–262. <https://doi.org/10.1083/jcb.94.2.253>.
- Soprano DR, Teets BW, Soprano KJ. 2007. Role of retinoic acid in the differentiation of embryonal carcinoma and embryonic stem cells. *Vitam Horm* 75:69–95. [https://doi.org/10.1016/S0083-6729\(06\)75003-8](https://doi.org/10.1016/S0083-6729(06)75003-8).
- Al Tanoury Z, Piskunov A, Andriamratsiresy D, Gaouar S, Lutzing R, Ye T, Jost B, Keime C, Rochette-Egly C. 2014. Genes involved in cell adhesion and signaling: a new repertoire of retinoic acid receptor target genes in mouse embryonic fibroblasts. *J Cell Sci* 127:521–533. <https://doi.org/10.1242/jcs.131946>.
- Mahony S, Mazzoni EO, McCuine S, Young RA, Wichterle H, Gifford DK. 2011. Ligand-dependent dynamics of retinoic acid receptor binding during early neurogenesis. *Genome Biol* 12:R2. <https://doi.org/10.1186/gb-2011-12-1-r2>.
- Balmer JE, Blomhoff R. 2002. Gene expression regulation by retinoic acid. *J Lipid Res* 43:1773–1808. <https://doi.org/10.1194/jlr.R100015-JLR200>.
- de Zulueta P, Alexandre E, Jacq B, Kerridge S. 1994. Homeotic complex and teashirt genes co-operate to establish trunk segmental identities in *Drosophila*. *Development* 120:2287–2296.
- Ragancokova D, Rocca E, Oonk AM, Schulz H, Rohde E, Bednarsch J, Feenstra I, Pennings RJ, Wendt H, Garratt AN. 2014. TSHZ1-dependent gene regulation is essential for olfactory bulb development and olfaction. *J Clin Invest* 124:1214–1227. <https://doi.org/10.1172/JCI72466>.
- Messeguer X, Escudero R, Farre D, Nunez O, Martinez J, Alba MM. 2002. PROMO: detection of known transcription regulatory elements using species-tailored searches. *Bioinformatics* 18:333–334. <https://doi.org/10.1093/bioinformatics/18.2.333>.
- Wu L, Timmers C, Maiti B, Saavedra HI, Sang L, Chong GT, Nuckolls F, Giangrande P, Wright FA, Field SJ, Greenberg ME, Orkin S, Nevins JR, Robinson ML, Leone G. 2001. The E2F1-3 transcription factors are essential for cellular proliferation. *Nature* 414:457–462. <https://doi.org/10.1038/35106593>.
- Julian LM, Blais A. 2015. Transcriptional control of stem cell fate by E2Fs and pocket proteins. *Front Genet* 6:161. <https://doi.org/10.3389/fgene.2015.00161>.
- Fajas L, Landsberg RL, Huss-Garcia Y, Sardet C, Lees JA, Auwerx J. 2002. E2Fs regulate adipocyte differentiation. *Dev Cell* 3:39–49. [https://doi.org/10.1016/S1534-5807\(02\)00190-9](https://doi.org/10.1016/S1534-5807(02)00190-9).
- Asp P, Acosta-Alvear D, Tsikitis M, van Oevelen C, Dynlacht BD. 2009. E2f3b plays an essential role in myogenic differentiation through isoform-specific gene regulation. *Genes Dev* 23:37–53. <https://doi.org/10.1101/gad.1727309>.
- Kim SY, Rane SG. 2011. The Cdk4-E2f1 pathway regulates early pancreas development by targeting Pdx1+ progenitors and Ngn3+ endocrine precursors. *Development* 138:1903–1912. <https://doi.org/10.1242/dev.061481>.
- Andrusiak MG, McClellan KA, Dugal-Tessier D, Julian LM, Rodrigues SP, Park DS, Kennedy TE, Slack RS. 2011. Rb/E2F regulates expression of neogenin during neuronal migration. *Mol Cell Biol* 31:238–247. <https://doi.org/10.1128/MCB.00378-10>.
- Ghanem N, Andrusiak MG, Svoboda D, Al Lafi SM, Julian LM, McClellan KA, De Repentigny Y, Kothary R, Ekker M, Blais A, Park DS, Slack RS. 2012. The Rb/E2F pathway modulates neurogenesis through direct regulation of the Dlx1/Dlx2 bigene cluster. *J Neuroscience* 32:8219–8230. <https://doi.org/10.1523/JNEUROSCI.1344-12.2012>.
- Rubin SM, Gall AL, Zheng N, Pavletich NP. 2005. Structure of the Rb C-terminal domain bound to E2F1-DP1: a mechanism for phosphorylation-induced E2F release. *Cell* 123:1093–1106. <https://doi.org/10.1016/j.cell.2005.09.044>.
- Dyson N. 1998. The regulation of E2F by pRB-family proteins. *Genes Dev* 12:2245–2262. <https://doi.org/10.1101/gad.12.15.2245>.
- Weinberg RA. 1995. The retinoblastoma protein and cell cycle control. *Cell* 81:323–330. [https://doi.org/10.1016/0092-8674\(95\)90385-2](https://doi.org/10.1016/0092-8674(95)90385-2).
- Kato J, Matsushime H, Hiebert SW, Ewen ME, Sherr CJ. 1993. Direct binding of cyclin D to the retinoblastoma gene product (pRb) and pRb phosphorylation by the cyclin D-dependent kinase CDK4. *Genes Dev* 7:331–342. <https://doi.org/10.1101/gad.7.3.331>.
- Ewen ME, Sluss HK, Sherr CJ, Matsushime H, Kato J, Livingston DM. 1993. Functional interactions of the retinoblastoma protein with mammalian D-type cyclins. *Cell* 73:487–497. [https://doi.org/10.1016/0092-8674\(93\)90136-E](https://doi.org/10.1016/0092-8674(93)90136-E).
- Magri L, Swiss VA, Jablonska B, Lei L, Pedre X, Walsh M, Zhang W, Gallo V, Canoll P, Casaccia P. 2014. E2F1 coregulates cell cycle genes and chromatin components during the transition of oligodendrocyte progenitors from proliferation to differentiation. *J Neurosci* 34:1481–1493. <https://doi.org/10.1523/JNEUROSCI.2840-13.2014>.
- Polager S, Kalma Y, Berkovich E, Ginsberg D. 2002. E2Fs up-regulate expression of genes involved in DNA replication, DNA repair and mitosis. *Oncogene* 21:437–446. <https://doi.org/10.1038/sj.onc.1205102>.
- Ren B, Cam H, Takahashi Y, Volkert T, Terragni J, Young RA, Dynlacht BD. 2002. E2F integrates cell cycle progression with DNA repair, replication, and G(2)/M checkpoints. *Genes Dev* 16:245–256. <https://doi.org/10.1101/gad.949802>.
- Cam H, Dynlacht BD. 2003. Emerging roles for E2F: beyond the G₁/S transition and DNA replication. *Cancer Cell* 3:311–316. [https://doi.org/10.1016/S1535-6108\(03\)00080-1](https://doi.org/10.1016/S1535-6108(03)00080-1).
- Cooper-Kuhn C, Vroemen M, Brown J, Ye H, Thompson M, Winkler J, Kuhn H. 2002. Impaired adult neurogenesis in mice lacking the transcription factor E2F1. *Mol Cell Neurosci* 21:312–323. <https://doi.org/10.1006/mcne.2002.1176>.
- Denechaud PD, Lopez-Mejia IC, Giral A, Lai Q, Blanchet E, Delacuisine B, Nicolay BN, Dyson NJ, Bonner C, Pattou F, Annicotte JS, Fajas L. 2016. E2F1 mediates sustained lipogenesis and contributes to hepatic steatosis. *J Clin Invest* 126:137–150. <https://doi.org/10.1172/JCI81542>.
- Poppy Roworth A, Ghari F, La Thangue NB. 2015. To live or let die—complexity within the E2F1 pathway. *Mol Cell Oncol* 2:e970480. <https://doi.org/10.4161/23723548.2014.970480>.
- Khair TB, Lund AH. 2010. Epigenetic dynamics across the cell cycle. *Essays Biochem* 48:107–120. <https://doi.org/10.1042/bse0480107>.
- Raum JC, Soleimanpour SA, Groff DN, Core N, Fasano L, Garratt AN, Dai C, Powers AC, Stoffers DA. 2015. Tshz1 regulates pancreatic beta-cell maturation. *Diabetes* 64:2905–2914. <https://doi.org/10.2337/db14-1443>.
- Erlik T, Li X, Courgeon M, Bertet C, Chen ZQ, Baumert R, Ng J, Koo C, Arain U, Behnia R, Rodriguez AD, Senderowicz L, Negre N, White KP, Desplan C. 2017. Integration of temporal and spatial patterning generates neural diversity. *Nature* 541:365–370. <https://doi.org/10.1038/nature20794>.
- McBurney MW, Reuhl KR, Ally AI, Nasipuri S, Bell JC, Craig J. 1988. Differentiation and maturation of embryonal carcinoma-derived neurons in cell culture. *J Neurosci* 8:1063–1073. <https://doi.org/10.1523/JNEUROSCI.08-03-01063.1988>.